IJASS

International Journal of
Aeronautical and Space Sciences

Time-varying modal parameters identification of large flexible spacecraft using a recursive algorithm

Zhiyu Ni*

State Key Laboratory of Robotics, Shenyang Institute of Automation, Chinese Academy of Sciences, Shenyang 110016, China
School of Aeronautics and Astronautics, Dalian University of Technology, Dalian 116024, China

Zhigang Wu** and Shunan Wu***

State Key Laboratory of Structural Analysis for Industrial Equipment, School of Aeronautics and Astronautics, Dalian University of Technology, Dalian 116024, China

Abstract

In existing identification methods for on-orbit spacecraft, such as eigensystem realization algorithm (ERA) and subspace method identification (SMI), singular value decomposition (SVD) is used frequently to estimate the modal parameters. However, these identification methods are often used to process the linear time-invariant system, and there is a lower computation efficiency using the SVD when the system order of spacecraft is high. In this study, to improve the computational efficiency in identifying time-varying modal parameters of large spacecraft, a faster recursive algorithm called fast approximated power iteration (FAPI) is employed. This approach avoids the SVD and can be provided as an alternative spacecraft identification method, and the latest modal parameters obtained can be applied for updating the controller parameters timely (e.g. the self-adaptive control problem). In numerical simulations, two large flexible spacecraft models, the Engineering Test Satellite-VIII (ETS-VIII) and Soil Moisture Active/Passive (SMAP) satellite, are established. The identification results show that this recursive algorithm can obtain the time-varying modal parameters, and the computation time is reduced significantly.

Key words: modal parameter identification; large flexible spacecraft; linear time-varying system; recursive subspace algorithm

1. Introduction

On-orbit identification experiments of spacecrafts that determine the modal parameters have been performed in some studies [1-3], such as the Galileo spacecraft and Hubble space telescope [4-5]. However, these identification experiments are mostly based on the linear time-invariant (LTI) system. From the perspective of actual operations, the configuration properties of these rigid-flexible coupling spacecrafts may be changed in orbit for many reasons, such as antenna rotation [6], reflector deployment [7], docking with another spacecraft [8] or capturing another moving body. Therefore, it is necessary to accurately identify the modal

parameters for the spacecraft when the system is linear time varying (LTV).

In existing identification algorithm for on-orbit spacecraft, the eigensystem realization algorithm (ERA) was mostly often used for the identification of modal parameters [1-5, 9-10]. The ERA is a typical system realization method. This approach constructs the Hankel matrix and utilizes singular value decomposition (SVD) at each time step to extract the observability matrix. Then, the system modal parameters and state-space model matrices {A, B, C} are determined. However, the ERA was mainly based on the time-invariant and slow time-varying system [1-4, 11]. For common time-varying system, the ERA is not always suitable.

(cc)   * Ph. D
     ** Professor, Corresponding author: wuzhg@dlut.edu.cn
     *** Ph. D

(184~194)15-128.indd   184   2016-07-05   오후 7:59:45

In this case, pseudo modal method based on multiple sets of experimental data was developed to estimate the time-varying system modal parameters [12-13]. The method assumed that multiple experiments are implemented in system identification, and the system undergoes the same time-varying change by a different input in each experiment. The pseudo modal method constructs an instantaneous Hankel matrix at each time step from the input and output (I-O) data sequences. By decomposing the Hankel matrix, the observability and controllability matrices are extracted. The time-varying modal parameters (pseudo modal) and the state-space matrices are derived from the observability and controllability matrices [12-14]. The pseudo modal method shows a good stability for noise disturbance. However, because multiple sets of experimental data and SVD are used, when the system order is high, the dimension of the Hankel matrix and corresponding computation complexity of SVD are large. Some control problems, such as the self-adaptive control, often need to obtain the latest dynamic parameters for updating the controller parameters in real time. In addition, the identified system parameters can help to track and monitor the on-orbit working condition of spacecraft. Consequently, looking for a faster identification method for spacecraft is useful.

In this paper, we attempt to provide an alternative method that differs from the commonly used identification methods, which are based on SVD, to determine the time-varying modal parameters recursively. A recursive subspace-tracking algorithm based on the projection approximation hypothesis called fast approximated power iteration (FAPI) [15] is applied. The recursive algorithm is considered as an unconstrained optimization problem. When the initial values are selected, the time-varying observability matrix at each time instant can be tracked by updating the I-O data in real time. Therefore, the FAPI method does not need to perform SVD for a Hankel matrix at each time step and is suitable for the on-line identification. The FAPI algorithm has been applied in some fields such as signal processing and mechanical engineering, but few studies have investigated using the method to identify the spacecraft time-varying modal parameters. In this paper, the computational accuracy and computation cost of this recursive algorithm and the pseudo modal method [12-13] are compared. In numerical simulations, two large rigid-flexible coupling spacecraft models are established. The identified results show that the FAPI recursive algorithm offers the capability to determine the time-varying frequency parameters. A series of results under different simulation conditions illustrate that the

computation time of recursive algorithm is significantly lower than the pseudo modal method, and the identified accuracy is acceptable for high signal noise ratio (SNR) in identifying the time-varying modal parameters of large flexible spacecraft.

The paper is organized as follows. Section 2 simply reviews the dynamical equations of the rigid-flexible coupling spacecraft. The FAPI algorithm is introduced in Section 3. In Section 4, we will discuss the design of input and output signals, and the time-varying modal parameters are identified using FAPI method. In Section 5, the results of two simulation examples are presented that illustrate the effectiveness of the recursive algorithm. Some concluding remarks are offered in the last Section.

2. Equation description of the rigid-flexible coupling spacecraft

The rigid-flexible coupling spacecraft structures can be constructed in the form of a central rigid body with N large flexible appendages such as solar panels or antennas. It is worth noting that this paper does not consider the translational motion of on-orbit spacecraft, but is only concerned with the rotational motion of structure. And we suppose that the angular velocity $\dot{\psi}$ of the spacecraft is very small, namely, $\dot{\psi} \approx 0$, and the solar panels are rotating with a uniform rotational speed of $\dot{\theta}$. When a 3×1 dimensional control torque $\boldsymbol{u}(t)$ is applied to the central rigid body, the dynamical equations of the spacecraft with N appendages are described by (The detail procedure of modelling can be found in other studies [16-17].):

$$\boldsymbol{J}(t)\ddot{\boldsymbol{\psi}} + \sum_i \boldsymbol{F}_i(t)\ddot{\boldsymbol{\eta}}_i = \boldsymbol{u}(t) \tag{1}$$

$$\boldsymbol{F}_i^{\mathrm{T}}(t)\ddot{\boldsymbol{\psi}} + \ddot{\boldsymbol{\eta}}_i + 2\zeta_i\boldsymbol{\Omega}_i\dot{\boldsymbol{\eta}}_i + \boldsymbol{\Omega}_i^2\boldsymbol{\eta}_i = 0 \,, i = \left\{1, 2, ..., N\right\} \tag{2}$$

where $\boldsymbol{\eta}$ is modal coordinate of appendages; ζ and $\boldsymbol{\Omega}$ are the damping ratio and natural frequency of appendages, respectively. Matrix $\boldsymbol{F}$ is the coupling coefficient for the appendage vibration and spacecraft rotation. $\boldsymbol{J}$ is the rotation inertia matrix of the entire spacecraft. Select a state vector $\boldsymbol{\delta}$ as:

$$\boldsymbol{\delta} = \begin{bmatrix} \boldsymbol{\psi}^{\mathrm{T}} & \boldsymbol{\eta}_1^{\mathrm{T}} & \boldsymbol{\eta}_2^{\mathrm{T}} & \cdots & \boldsymbol{\eta}_i^{\mathrm{T}} \end{bmatrix}^{\mathrm{T}}, \quad i = \left\{1, 2, ..., N\right\} \tag{3}$$

and equations (1) and (2) can be expressed as:

$$\boldsymbol{M}(t)\ddot{\boldsymbol{\delta}} + \boldsymbol{E}\dot{\boldsymbol{\delta}} + \boldsymbol{K}\boldsymbol{\delta} = \boldsymbol{L}\boldsymbol{u}(t) \tag{4}$$

where

$$M(t) = \begin{bmatrix} J(t) & F_1(t) & \cdots & F_i(t) \\ F_1^{\mathrm{T}}(t) & I_{\kappa \times \kappa} & & \\ \vdots & & \ddots & \\ F_i^{\mathrm{T}}(t) & & & I_{\kappa \times \kappa} \end{bmatrix},$$

$$E = \begin{bmatrix} \mathbf{0}_{3 \times 3} & & & \\ & 2\zeta_1 \boldsymbol{\Omega}_1 & & \\ & & \ddots & \\ & & & 2\zeta_i \boldsymbol{\Omega}_i \end{bmatrix}, K = \begin{bmatrix} \mathbf{0}_{3 \times 3} & & & \\ & \boldsymbol{\Omega}_1^2 & & \\ & & \ddots & \\ & & & \boldsymbol{\Omega}_i^2 \end{bmatrix},$$

$$L = \begin{bmatrix} I_{3 \times 3} \\ \mathbf{0}_{\sum_i \kappa \times 3} \end{bmatrix} \quad i = \{1, 2, \ldots, N\}$$

where I is an identity matrix and κ denotes the number of selected vibration modes for each appendage. Then the state equation can be established as:

$$\dot{x}(t) = A(t)x(t) + B(t)u(t) \tag{5}$$

where $x(t)$ is the $n \times 1$ dimensional state vector; $A(t)$ and $B(t)$ are the $n \times n$ system matrix and $n \times r$ input matrix respectively as follows:

$$A(t) = \begin{bmatrix} \mathbf{0} & I \\ -M^{-1}(t)K & -M^{-1}(t)E \end{bmatrix}, \quad B(t) = \begin{bmatrix} \mathbf{0} \\ M^{-1}(t)L \end{bmatrix}$$

The $m \times 1$ dimensional satellite output signal $y(t)$ is selected as $y(t) = \left[\psi^{\mathrm{T}}, s^{\mathrm{T}}, \dot{\psi}^{\mathrm{T}}, \dot{s}^{\mathrm{T}} \right]$, where s is the vibration displacement of appendage. The measurement equation of satellite can be written as:

$$y(t) = Cx(t) = \begin{bmatrix} H & \\ & H \end{bmatrix} \begin{bmatrix} \delta \\ \dot{\delta} \end{bmatrix} \tag{6}$$

where C is the $m \times n$ output matrix, the form of the matrix H is follows:

$$H = \begin{bmatrix} I & \\ & \boldsymbol{\Phi}_i \end{bmatrix}, \quad i = \{1, 2, \ldots, N\}$$

and matrix $\boldsymbol{\Phi}$ is the modal matrix of appendages.

3. Review of the FAPI algorithm

The discrete form of equations (5) and (6) with process and measurement noises can be described as:

$$x(k+1) = A(k)x(k) + B(k)u(k) + w_n(k) \tag{7}$$

$$y(k) = C(k)x(k) + v_n(k) \tag{8}$$

and the I-O data sequences at time step k are described by:

$$u_M(k) = \begin{bmatrix} u^{\mathrm{T}}(k) & u^{\mathrm{T}}(k+1) & \cdots & u^{\mathrm{T}}(k+M-1) \end{bmatrix}^{\mathrm{T}} \tag{9}$$

$$y_M(k) = \begin{bmatrix} y^{\mathrm{T}}(k) & y^{\mathrm{T}}(k+1) & \cdots & y^{\mathrm{T}}(k+M-1) \end{bmatrix}^{\mathrm{T}} \tag{10}$$

Therefore, equations (7) and (8) can be written as:

$$y_M(k) = \boldsymbol{\Gamma}(k)x(k) + \Delta(k)u_M(k) + V_n(k) \tag{11}$$

where

$$\boldsymbol{\Gamma}(k) = \begin{bmatrix} C(k) \\ C(k+1)A(k) \\ \vdots \\ C(k+M-1)A(k+M-2)\ldots A(k) \end{bmatrix}$$

$$\Delta(k) = \begin{bmatrix} \mathbf{0} & & & \\ C(k+1)B(k) & \mathbf{0} & & \\ \vdots & \vdots & & \ddots \\ C(k+M-1)A(k+M-2)\cdots B(k) & C(k+M-1)A(k+M-2)\cdots B(k+1) & \cdots & \mathbf{0} \end{bmatrix}$$

and $V_n(k)$ is the noise item in equation. Define a random vector ξ and the following unconstrained criterion is considered:

$$J(\boldsymbol{\Gamma}(k)) = \mathrm{E} \left\| \xi(k) - \boldsymbol{\Gamma}(k)\boldsymbol{\Gamma}^{\mathrm{T}}(k)\xi(k) \right\|^2 \tag{12}$$

Assuming that the observability matrix $\boldsymbol{\Gamma}(k)$ is full rank, and define the self-correlations matrix $R_{\xi\xi}$ of vector $\xi(k)$ as:

$$R_{\xi\xi}(k) = \mathrm{E}[\xi(k)\xi^{\mathrm{T}}(k)] \tag{13}$$

If the expectation shown in equation (12) is replaced with the exponentially weighted summation, then the following is true [15]:

$$J(\boldsymbol{\Gamma}(k)) = \sum_{i=1}^{k} \beta^{k-i} \left\| \xi(i) - \boldsymbol{\Gamma}(k)\boldsymbol{\Gamma}^{\mathrm{T}}(k)\xi(i) \right\|^2 \tag{14}$$

where β is the forgetting factor. According to the theorem of global minimum of $J(\boldsymbol{\Gamma}(k))$, equation (13) can be replaced by:

$$R_{\xi\xi} = \sum_{i=1}^{k} \beta^{k-i} \xi(i)\xi^{\mathrm{T}}(i) \tag{15}$$

In equation (14), the primary idea of the FAPI method is to construct a subspace projection approximation using:

$$h(k) = \boldsymbol{\Gamma}^{\mathrm{T}}(k-1)\xi(k) \tag{16}$$

To minimize $J(\boldsymbol{\Gamma}(k))$ in equation (14), equation (16) is applied, and a modified cost function is follows:

$$J'(\boldsymbol{\Gamma}(k)) = \sum_{i=1}^{k} \beta^{k-i} \left\| \xi(i) - \boldsymbol{\Gamma}(k)h(i) \right\|^2 \tag{17}$$

which is quadratic in the elements of $\boldsymbol{\Gamma}(k)$. $J'(\boldsymbol{\Gamma}(k))$ is

minimized if:

$$\boldsymbol{\Gamma}(k) = \boldsymbol{R}_{\xi h}(k)\boldsymbol{R}_{hh}^{-1}(k) \tag{18}$$

Define a modified matrix $\boldsymbol{\Theta}(k)$ as:

$$\boldsymbol{\Gamma}(k) = \boldsymbol{\Gamma}(k-1)\boldsymbol{\Theta}(k) \tag{19}$$

When the matrix inversion lemma is applied to equation (18), a recursive format of $\boldsymbol{\Gamma}(k)$ is derived as:

$$\boldsymbol{\Gamma}(k) = (\boldsymbol{\Gamma}(k-1) + \boldsymbol{e}(k)\boldsymbol{g}^{\mathrm{T}}(k))\boldsymbol{\Theta}(k) \tag{20}$$

with $\boldsymbol{e}(k) = \boldsymbol{\xi}(k) - \boldsymbol{\Gamma}(k-1)\boldsymbol{h}(k)$ and
$\boldsymbol{g}(k) = \boldsymbol{Z}(k-1)\boldsymbol{h}(k)(\beta + \boldsymbol{h}^{\mathrm{T}}(k)\boldsymbol{Z}(k-1)\boldsymbol{h}(k))^{-1}$. $\boldsymbol{Z}(k)$ is derived from a suitable initial value $\boldsymbol{Z}(0)$ recursively.

Calculating the matrix $\boldsymbol{\Theta}(k)$ and substituting it to equation (20) yields:

$$\boldsymbol{\Gamma}(k) = \boldsymbol{\Gamma}(k-1) + \boldsymbol{e}'(k)\boldsymbol{g}^{\mathrm{T}}(k) \tag{21}$$

where

$$\boldsymbol{e}'(k) = (1 - \boldsymbol{\tau}(k)\|\boldsymbol{g}(k)\|^2)\boldsymbol{e}(k) - \boldsymbol{\tau}(k)\boldsymbol{\Gamma}(k-1)\boldsymbol{g}(k)$$

$$\boldsymbol{\tau}(k) = \|\boldsymbol{e}(k)\|^2 / (1 + \|\boldsymbol{e}(k)\|^2 \|\boldsymbol{g}(k)\|^2 + \sqrt{1 + \|\boldsymbol{e}(k)\|^2 \|\boldsymbol{g}(k)\|^2})$$

The detailed theory description of the FAPI algorithm was introduced in reference [15, 18], so we will not discuss the derivation of this method again. Table 1 shows the procedures of FAPI. The computational cost of this recursive algorithm is $4mMn+O(n^2)$ flops per iteration, whereas the complexities of the common-used identification method, which is based on SVD, is $O(n^3)$ at least. Therefore, the computational cost of FAPI is lower than the SVD method. Particularly, when the order of spacecraft system is high, the advantage of computational efficiency for the recursive algorithm is obvious. Applying this projection approximation, the matrix $\boldsymbol{\Gamma}(k)$ of the time-varying system can be derived.

In FAPI algorithm, we need to apply the I-O data $\boldsymbol{u}(k)$ and $\boldsymbol{y}(k)$ to construct the vector $\boldsymbol{\xi}(k)$ of the FAPI algorithm. For this purpose, a data pre-processing way to construct and update the vector $\boldsymbol{\xi}(k)$ is introduced in Appendix A.

4. Identification of time-varying modal parameters

In this section, the design of input and output signals for spacecraft identification is considered. By the FAPI method, the system time-varying modal parameters (e.g. frequency and damping ratio) are estimated from the observability

matrix.

4.1 Design of input and output signals

To simulate the control torque signal $\boldsymbol{u}(t)$ produced by reaction wheel, the approximate square signal will be applied in this paper. Considering the loading and unloading process of torque with time, the designed torque input signal $\boldsymbol{u}(t)$ for the simulations is shown in Fig. 1, where the maximum value $\boldsymbol{u}_{\max}(t)$=2 Nm.

For the output signal $\boldsymbol{y}(t)$ in equation (6), the attitude angle and attitude angular velocity can be measured by the gyros and earth/sun sensors in central rigid body of spacecraft. Besides the attitude signals, the vibration signals of spacecraft appendages are also needed in this paper. Otherwise, some orders of frequency may not be identified accurately.

Optimal sensor placement for the identification and control of large dynamic structures can be studied as a separate problem. Here we only consider the simplest sensor placement situation: only the out-of-plane vibration response signals of some nodes on each appendage are selected, and the sensors are placed at the end and the edge

Table 1. FAPI algorithm

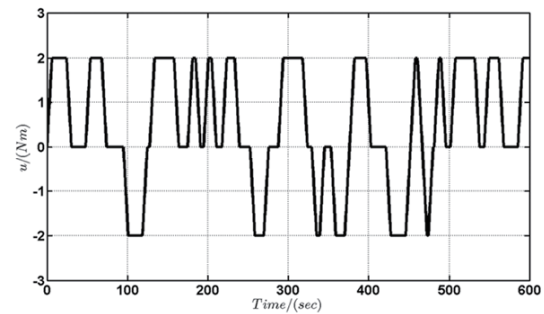| |
|---|
| **Initialization**: |
| $\boldsymbol{\Gamma}(0) = \begin{bmatrix} \boldsymbol{I}_n \\ \boldsymbol{0}_{(mM-n)\times n} \end{bmatrix}, \boldsymbol{Z}(0) = \boldsymbol{I}_n$ |
| For k=1,2,3,…: |
| $\quad \boldsymbol{h}(k) = \boldsymbol{\Gamma}^{\mathrm{T}}(k-1)\boldsymbol{\xi}(k)$ |
| $\quad \boldsymbol{v}(k) = \boldsymbol{Z}(k-1)\boldsymbol{h}(k)$ |
| $\quad \boldsymbol{g}(k) = \boldsymbol{v}(k)(\beta + \boldsymbol{h}^{\mathrm{T}}(k)\boldsymbol{v}(k))^{-1}$ |
| $\quad \boldsymbol{e}(k) = \boldsymbol{\xi}(k) - \boldsymbol{\Gamma}(k-1)\boldsymbol{h}(k)$ |
| $\quad \boldsymbol{\tau}(k) = \|\boldsymbol{e}(k)\|^2 / (1 + \|\boldsymbol{e}(k)\|^2 \|\boldsymbol{g}(k)\|^2 + \sqrt{1 + \|\boldsymbol{e}(k)\|^2 \|\boldsymbol{g}(k)\|^2})$ |
| $\quad \boldsymbol{v}'(k) = \boldsymbol{Z}^{\mathrm{T}}(k-1)((1 - \boldsymbol{\tau}(k)\|\boldsymbol{g}(k)\|^2)\boldsymbol{h}(k) + \boldsymbol{\tau}(k)\boldsymbol{g}(k))$ |
| $\quad \boldsymbol{\varepsilon}(k) = (\boldsymbol{\tau}(k)\boldsymbol{Z}(k-1)\boldsymbol{g}(k) - \boldsymbol{\tau}(k)\boldsymbol{v}'^{\mathrm{T}}(k)\boldsymbol{g}(k)\boldsymbol{g}(k)) / (1 - \boldsymbol{\tau}(k)\|\boldsymbol{g}(k)\|^2)$ |
| $\quad \boldsymbol{Z}(k) = (\boldsymbol{Z}(k-1) - \boldsymbol{g}(k)\boldsymbol{v}'^{\mathrm{T}}(k) + \boldsymbol{\varepsilon}(k)\boldsymbol{g}^{\mathrm{T}}(k)) / \beta$ |
| $\quad \boldsymbol{e}'(k) = (1 - \boldsymbol{\tau}(k)\|\boldsymbol{g}(k)\|^2)\boldsymbol{e}(k) - \boldsymbol{\tau}(k)\boldsymbol{\Gamma}(k-1)\boldsymbol{g}(k)$ |
| $\quad \boldsymbol{\Gamma}(k) = \boldsymbol{\Gamma}(k-1) + \boldsymbol{e}'(k)\boldsymbol{g}^{\mathrm{T}}(k)$ |

Fig. 1. Designed torque input signal

of appendages. (The detailed placement situations see the simulation examples in the subsequent section).

4.2 Identification of time-varying modal parameters

For the identified matrix $\Gamma(k)$ by the FAPI algorithm, the system matrix $A(k)$ can be constructed as:

$$A(k) = [\Gamma_1(k+1)]^{\dagger}[\Gamma_2(k)] \tag{22}$$

where $\Gamma_1(k+1)$ and $\Gamma_2(k)$ are the first $m\times(M-1)$ rows of $\Gamma(k+1)$ and the last $m\times(M-1)$ rows of $\Gamma(k)$, respectively. The notation " $\dagger$ " denotes the Moore-Penrose inverse.

If the system matrix $A(k)$ has been derived, the identification of the time-varying modal parameters of the spacecraft can be implemented. The eigenvalue decomposition of the system matrix $A(k)$ is [12]:

$$A(k) = \Lambda(k)\Sigma(k)\Lambda^{-1}(k) \tag{23}$$

where $\Sigma(k)$ is the diagonal eigenvalue matrix, $\Sigma(k) = \text{diag}(\lambda_1(k), \lambda_2(k), \ldots, \lambda_n(k))$, in which $\lambda_j(k)(j=1, 2, \cdots, \text{n})$ contains time-varying conjugate complex eigenvalues; and $\Lambda(k)$ is a time-varying matrix of eigenvectors. The jth pseudo eigenvalue is $\lambda_j(k) = \exp(-\varsigma_j(k)\Delta t \pm i\omega_j(k)\Delta t)$, in which $-\varsigma_j(k)$ and $\omega_j(k)$ are referred to as the jth system pseudo-damping ratio and pseudo-damped natural frequency, respectively; Δt is the sampled time, and $i = \sqrt{-1}$.

4.3 Summary of identification procedures

Step 1: Using the I-O data sequences $u_M(k)$ and $y_M(k)$ in equations (9)-(10), the data vector $\xi(k)$ is determined by the data pre-processing method described in Appendix A from equations (A.4), (A.9), (A.11) and (A.12).

Step 2: The identified observability matrix $\Gamma(k)$ is obtained from the data vector $\xi(k)$ by the FAPI algorithm described in Section 3.

Step 3: The time-varying frequency (pseudo modal frequency) and damping ratio of the spacecraft can be determined from equation (23) by the eigenvalue

decomposition.

5. Simulation Examples

In the following, two numerical simulation models of large flexible spacecraft are established. The time-varying modal parameters are identified by the recursive algorithm.

5.1 Large flexible satellite ETS-VIII

The Engineering Test Satellite-VIII (ETS-VIII) spacecraft was launched in 2006 by Japan to provide digital communications for mobile telephones and other mobile devices. It is a geosynchronous satellite at an altitude of approximately 35,786 km. The satellite has four large flexible appendages including a pair of deployable antenna reflectors and a pair of solar array panels [19]. The solar panels rotate around the pitch axis so that they continually face the sun; the solar panel rotation of the satellite can cause a maximum 25% change for the structure parameters [20]. Consequently, the satellite can be studied as an LTV system.

We simplify the satellite model based on the following conditions: the antenna reflectors are considered to be a plane truss structure, and the centre rigid body of the satellite is considered to be a solid cuboid. The panels and reflectors are hinged with centre rigid body by a linkage. The four appendages are composed of a homogeneous material. The gravitational gradient torque is omitted here because ETS-VIII is a geosynchronous satellite. Selecting the entire satellite's centre of mass as the coordinate origin, and the origin of each appendage coordinate is established at the hinge joint of centre rigid body and appendage. The simplified satellite configuration and the sensor placement on appendages are shown in Fig. 2(a), and the size of the satellite model is shown in Fig. 2(b), where we use the notations {s1,s2,a1,a2} to denote the north/south solar panels and the A/B antenna reflector, respectively.
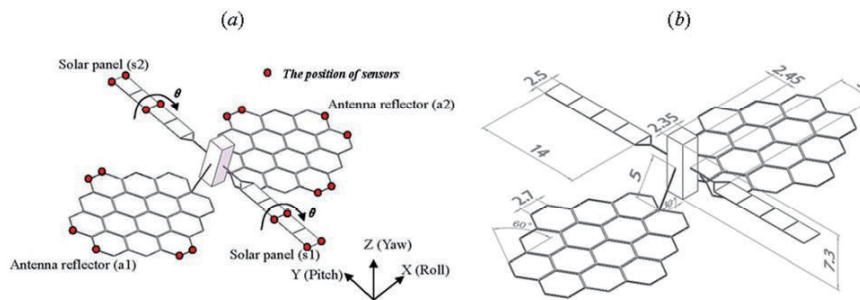
The frequencies of panels s1/s2 and antennas a1/a2

Fig. 2. Simplified ETS-VIII model (unit: m)

188

are obtained by finite element modeling (FEM) and the damping ratio $\zeta_{s1}=\zeta_{s2}=\zeta_{s3}=\zeta_{s4}=0.01$. In these simulations, we select first four frequencies for each appendage, namely $\kappa=4$ in equation (4). Therefore, the order of the satellite system is $n=(3+4\times4)\times2=38$. The rotation speed $\dot{\theta}$ of the solar panels are selected as $\dot{\theta}=0.6$ deg/s. The parameters of the recursive algorithm are given as follows: system sampling interval $\Delta t=0.01$ s, the Hankel matrix parameter $M=20$ to make sure the rank of Hankel matrix is larger than the system order. From past experience, the forgetting factor is usually selected as $0.95\leq\beta<1$ in recursive algorithm, so the forgetting factor $\beta=0.98$ in this simulation. The measurement noise is a stationary zero-mean Gaussian random noise, and the SNR is selected as 50 dB. We only discuss the system identification in the open-loop system for simplicity. The closed-loop identification situation will be discussed in another article.

The original frequencies for the established satellite model are shown in Fig. 3, where the first three frequencies are zero because these correspond to three rigid modes of the satellite. In addition to these three rigid frequencies, the first five vibration frequencies from 4th to 8th are selected. Applying the recursive algorithm, the frequencies of ETS-VIII can be obtained. Fig. 4(a) compares the results of the time-invariant 4th and 6th to 7th frequencies between the original and identified values by the recursive algorithm. Fig. 4(b) shows the time-varying 5th and 8th frequency values computed by the recursive method. From Fig. 4, it can be seen that the recursive algorithm can track and obtain the time-varying frequency values.

In this simulation example, in addition to the FAPI

recursive algorithm, the pseudo modal method is also applied to identify the time-varying frequencies. The average relative errors of each frequency are shown in Table 2. (Implement 30 experiments for each approach) The error results show that both the recursive algorithm and pseudo modal method can identify the time-varying frequencies. Although the relative error for recursive algorithm is slightly higher than the SVD method, the maximum error remains below 3%. The results of Table 2 show that the recursive algorithm can be applied to identify the time-varying modal parameters of spacecraft.

In aforementioned numerical simulations, the system order n is small, only $(3+4\times4)\times2=38$. However, the system order of spacecraft model is higher in practice. Therefore, the computational efficiency of these two methods is compared. Now we consider the situations for different system orders: the orders of system model are selected as 70, 110 and 150,
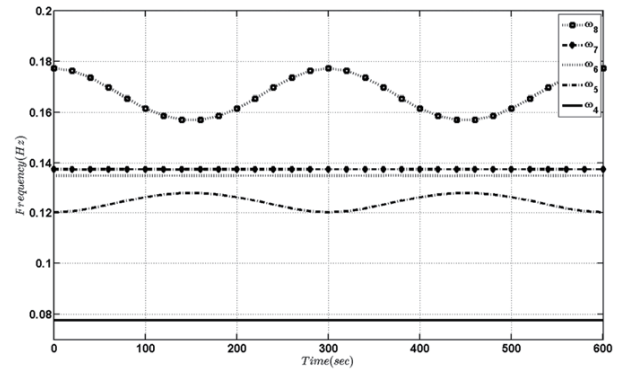

Fig. 3. The original 4th to 8th frequencies of the established ETS-VIII model
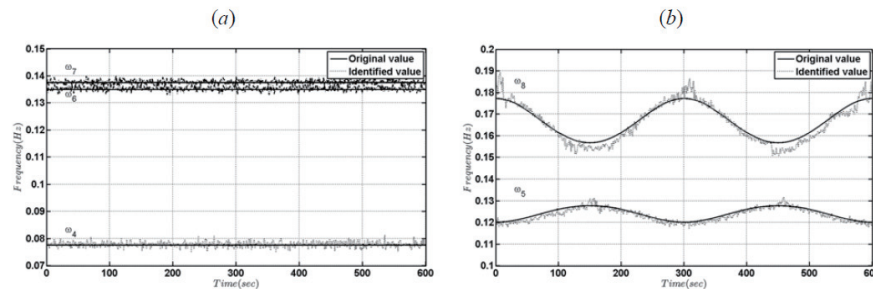

Fig. 4. Identification results of the frequencies of the ETS-VIII by the recursive algorithm (SNR=50)

Table 2. Error comparison of frequencies computed by the recursive algorithm and pseudo modal method (SNR=50)

Frequency	Recursive algorithm	Pseudo modal method
ω_4	1.9754%	1.8536%
ω_5	1.7590%	1.5795%
ω_6	1.4578%	1.2580%
ω_7	1.7236%	1.4547%
ω_8	2.1368%	1.7834%

respectively. The average computation time for the recursive and pseudo modal method is shown in Table 3, where the relative computation efficiency (RCE) e_{RCE} is defined as follows:

$$e_{RCE} = \frac{\left| \overline{t}_{pm} - \overline{t}_r \right|}{\overline{t}_{pm}} \times 100\% \qquad (24)$$

where $\overline{t}_{pm}$ and $\overline{t}_r$ are the average computation time using the pseudo modal method and recursive algorithm, respectively. Then, the simulation results in Table 3 illustrate the conclusion of the computation complexity in Section 3: because SVD is required in the pseudo modal method, the computation time is found to be much larger than that of the recursive algorithm. Particularly, when the orders of system model increases, the difference of the relative computational efficiency e_{RCE} between these two methods is obvious, and the recursive algorithm has better computation speed in the identification of high-order model.

The identification of recursive method for different SNRs is also tested. The results of Table 4 illustrate that the recursive algorithm can track the time-varying modal parameters when the SNR is high (SNR>20 in this example). However, a lower SNR will affect the identified accuracy significantly.

5.2 SMAP satellite

In the second numerical example, an LTV model of the Soil Moisture Active/Passive (SMAP) satellite is provided. The SMAP mission is an observation mission proposed by the U.S. Jet Propulsion Laboratory to survey global soil moisture and freeze-thaw states [6]. The launch of this satellite can help to improve the accuracy of weather forecasting, flood warning, and drought monitoring. The Delta II rocket sent the satellite into a near-circular orbit

at perigee 660 km and apogee 685 km on January 31, 2015, U.S. Eastern Standard Time. To maximize the scope of earth observation during the satellite's in-orbit operation and obtain high-resolution global soil moisture maps, the on-board large deployable antenna can rotate at a speed of 4 s/r.

The simplified SMAP satellite model and the sensor placement of the appendages are shown in Fig. 5(a), and the size of the satellite model is illustrated in Fig. 5(b). Comparing with the rotation speed of the solar panels in Example 1, the rotational speed of antenna in this example is higher ($\dot{\theta}$=90 deg/sec). The first 4 orders and the first 8 orders of modal frequencies for solar panels and antenna are selected, respectively. Therefore, the order n of state-space equation (5) is n=(3+2×4+8)×2=38, the damping ratio of antenna for each order is selected as 0.05, and the damping ratio of panels for each order is selected as 0.1. In the established satellite model, the 1st to 3rd orders of frequencies denote the rigid body motion of the satellite and are equal to zero. The standard zero-mean Gaussian random noise is the process noise and measurement noise, respectively, and the SNRs for process and measurement noise are both selected as 50 dB.

The following parameters are provided in the numerical simulation: forgetting factor β=0.98, sampling time Δt=0.01 s, and the Hankel matrix parameter M=20. The time-varying frequency of the satellite is identified using the proposed recursive algorithm and pseudo modal method. The results of the 4th to 7th orders frequency values are shown in Fig. 6, and Table 5 shows the average relative errors of each frequency by these two approaches. Fig. 6 and Table 5 illustrate that these two methods can effectively identify the system frequencies under the high SNR.

Figure 7 shows the identification results of the 4th frequency

Table 3. Average computation time between these two methods for different system orders n (unit: s)

System order	Recursive algorithm	Pseudo modal method	e_{RCE}
n=38	41.56	72.06	42.33%
n=70	78.75	145.82	46.00%
n=110	101.43	216.33	53.11%
n=150	138.51	347.28	60.12%

Table 4. Error comparison of frequencies by the recursive algorithm for different measurement SNRs

Frequency	SNR=40	SNR=30	SNR=20	SNR=10
ω_4	2.3356%	2.8754%	7.5679%	10.7804%
ω_5	2.0860%	2.7774%	6.5678%	9.7903%
ω_6	1.8567%	2.4956%	4.4567%	7.5687%
ω_7	2.1426%	2.6574%	5.8467%	8.5674%
ω_8	2.5689%	3.1854%	8.2580%	11.5686%

190

using the recursive algorithm when the measurement noise is selected with different SNRs. The error comparisons of frequencies are presented in Table 6. As shown in Table 6, the results demonstrate that the computation accuracy is better when SNR≥30, and the relative error of the frequencies increases substantially when SNR≤20. Similar with the conclusion of Example 1, the simulation results prove that a lower SNR signal will dramatically affect the identified results.

Finally, the computational efficiency of the two methods is compared for different system orders in Table 7, where the orders of system model are selected as 50, 80 and 140, respectively. Similar with the results in Table 3, The e_{RCE} in

Table 7 illustrates that the recursive algorithm has better computation efficiency when the system order is high.
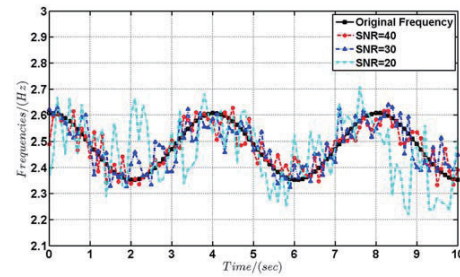

Fig. 7. Comparison of the 4th frequencies for different measurement SNRs using the recursive algorithm
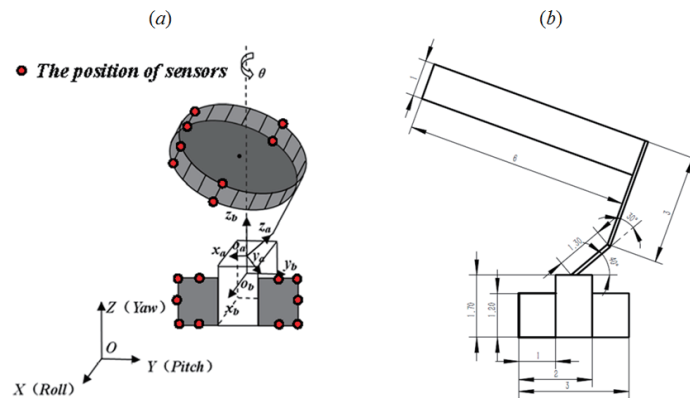

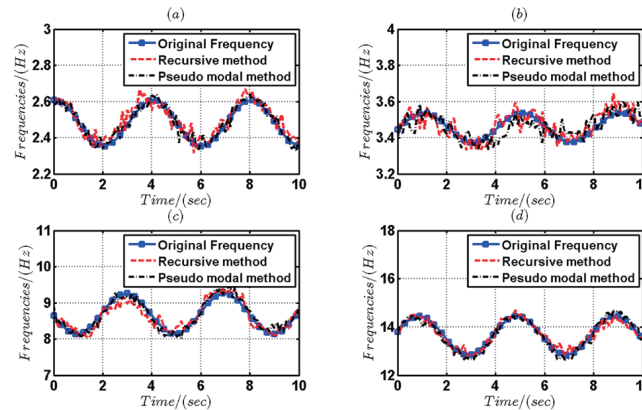Fig. 5. Simplified SMAP satellite model (unit: m)

Fig. 6. Identification results of the 4th to 7th frequencies of the SMAP satellite by the recursive algorithm: (a) the 4th frequency; (b) the 5th frequency; (c) the 6th frequency; (d) the 7th frequency (SNR=50)

Table 5. Error comparison of frequencies computed by the recursive algorithm and pseudo modal method (SNR=50)

Frequency	Recursive algorithm	Pseudo modal method
ω_4	1.6843%	1.4578%
ω_5	2.1245%	2.4567%
ω_6	1.4578%	1.4684%
ω_7	1.1256%	1.2356%

Table 6. Error comparison of frequencies by the recursive algorithm for different measurement SNRs

Frequency	SNR=40	SNR=30	SNR=20	SNR=10
ω_4	1.8689%	3.7257%	6.3449%	10.1023%
ω_5	2.8557%	4.7934%	8.9258%	13.9532%
ω_6	2.1674%	2.4941%	6.9278%	11.8532%
ω_7	2.2356%	2.6435%	7.4857%	10.6843%

Table 7. Average computation time between these two methods for different system orders *n* (unit: s)

System order	Recursive algorithm	Pseudo modal method	e_{RCE}
n=38	43.68	73.59	40.64%
n=50	53.24	94.61	43.73%
n=80	81.85	156.40	47.67%
n=140	128.37	304.42	57.83%

6. Conclusions

In this paper, we attempt to provide an alternative method that differs from commonly-used SVD approaches [12-13] to increase computational efficiency of modal parameters identification. For this purpose, considering the design of I-O data, the time-varying modal parameters of spacecraft system are determined by the FAPI recursive algorithm. Simulation results demonstrate that the recursive algorithm can satisfy identification accuracy and has better computational efficiency than the pseudo modal method which is based on SVD. Particularly, when the order of spacecraft system is high, the advantage of computational efficiency for the recursive method is remarkable in Tables 3 and 7.

In addition, the results of Tables 4 and 6 illustrate that when the SNR is high, the recursive algorithm is available for identifying the time-varying frequencies; but if the SNR is low, the identification precision becomes poor, and the algorithm is easily disturbed by noise. This is because the SVD is avoided in determining the observability matrix, and the noises have significant influence for the identified results. Therefore, how to improve the ability of noise immunity for the recursive algorithm, or whether some wave filtering methods may be used to reduce the effect of noise, are needed to be studied further.

Acknowledgement

References

[1] Yamaguchi, I., Kida, T., Komatsu, K., Sano, M., Sekiguchi, T., Ishikawa, S., Ichikawa, S., Yamada, K., Chida, Y. and Adachi, S., "ETS-VI On-Orbit System Identification Experiments", *JSME International Journal*, Vol. 40, No. 4, 1997, pp. 623-629.

DOI: 10.1299/jsmec.40.623

[2] Adachi, S., Yamaguchi, I., Kida, T., Sekiguchi, T., Yamada, K. and Chida, Y., "On-orbit System Identification Experiments on Engineering Test Satellite-VI", *Control Engineering Practice*, Vol. 7, No. 7, 1999, pp. 831-841.

DOI: 10.1016/s0967-0661(99)00032-5

[3] Kasai, T., Yamaguchi, I., Igawa, H., Mitani, S., Ohtani, T., Ikeda, M. and Sunagawa, K., "On-Orbit System Identification Experiments of the Engineering Test Satellite-VIII", *Transactions of the Japan Society for Aeronautical & Space Sciences Space Technology Japan*, Vol. 7, 2009, pp. 79-84.

DOI: 10.2322/tstj.7.pc_79

[4] Pappa, R. S. and Juang, J. N., "Galileo Spacecraft Modal Identification using An Eigensystem Realization Algorithm", *25th Structures, Structural Dynamics and Materials Conference*, Palm Springs, CA, USA, 1984.

DOI: 10.2514/6.1984-1070

[5] Juang, J. N., Phan, M., Horta, L. G. and Longman R. W., "Identification of Observer/Kalman Filter Markov Parameters: Theory and Experiments", *Journal of Guidance, Control and Dynamics*, Vol. 16, No. 2, 1993, pp. 320-329.

DOI: 10.2514/3.21006

[6] Entekhabi, D., Njoku, E. G., O'Neill, P. E., Kellogg, K. H., Crow, W. T., Edelstein W. N., Entin, J. K., Goodman, S. D., Jackson, T. J., Johnson, J., Kimball, J., Piepmeier, J. R., Koster, R. D., Martin, N., Mcdonald, K. C., Moghaddam, M., Moran,

S., Reichle, R., Shi, J. C., Spencer, M. W., Thurman, S. W., Tsang, L. and Van Zyl, J., "The Soil Moisture Active Passive (SMAP) Mission", *Proceedings of the IEEE*, Vol. 98, No. 5, 2010, pp. 704-716.

DOI: 10.1109/JPROC.2010.2043918

[7] Meguro, A., Shintate, K., Usui, M. and Tsujihata, A., "In-orbit Deployment Characteristics of Large Deployable Antenna Reflector Onboard Engineering Test Satellite VIII", *Acta Astronautica*, Vol. 65, No. 9, 2009, pp. 1306-1316.

DOI: 10.1016/j.actaastro.2009.03.052

[8] Kim, H. M. and Bokhour, E. B., "Mir Structural Dynamics Experiment: A Flight Experiment Development", *Proceedings of the 38th AIAA Structures, Structural Dynamics, and Materials Conference*, Kissimmee, Florida, UT USA, April, 1997.

DOI: 10.2514/6.1997-1169

[9] Yamaguchi, I., Kasai, T. and Igawa, H., "Multi-input Multi-output System Identification using Impulse Responses", *Journal of Space Engineering*, Vol. 1, No. 1, 2008, pp. 1-11.

DOI: 10.1299/spacee.1.1

[10] Cooper, J. and Wright, J., "Spacecraft In-orbit Identification using Eigensystem Realization Methods", *Journal of Guidance, Control and Dynamics*, Vol. 15, No. 2, 1992, pp. 352-359.

DOI: 10.2514/3.20843

[11] Yamaguchi, I., Kida, T. and Kasai, T., "Experimental Demonstration of LSS System Identification by Eigensystem Realization Algorithm", *Proceedings of American Control Conference* (Seattle, WA), American Automatic Control Council, Evanston, IL, 1995.

DOI: 10.1109/acc.1995.529279

[12] Liu, K. F. and Deng, L. Y., "Experimental Verification of an Algorithm for Identification of Linear Time-varying Systems", *Journal of Sound and Vibration*, Vol. 279, No. 3, 2005, pp. 1170-1180.

DOI: 10.1016/j.jsv.2004.01.040

[13] Liu, K. F. and Deng, L. Y., "Identification of Pseudo-natural Frequencies of an Axially Moving Cantilever Beam using A Subspace-based Algorithm", *Mechanical System and Signal Processing*, Vol. 20, No. 1, 2006, pp. 94-113.

DOI: 10.1016/j.ymssp.2004.10.003

[14] Shi, Z. Y., Law, S. S. and Li, H. N., "Subspace-based Identification of Linear Time-varying System", *AIAA Journal*, Vol. 45, No. 8, 2007, pp. 2042-2050.

DOI: 10.2514/1.28555

[15] Badeau, R., Richard, G., David, B. and Abed-Meraim, K., "Approximated Power Iterations for Fast Subspace Tracking", *IEEE 7th International Symposium on Signal Processing and Its Applications*, Vol. 2, 2003, pp. 583-586.

DOI: 10.1109/isspa.2003.1224944

[16] Hablani, H. B., "Constrained and Unconstrained Modes: Some Modeling Aspects of Flexible Spacecraft", *Journal of Guidance, Control and Dynamics*, Vol. 5, No. 2, 1982, pp. 164-173.

DOI: 10.2514/3.19764

[17] Craig, R. R., "Coupling of Substructures for Dynamic Analyses: An Overview", Collection of the 41st AIAA/ASME/ASCE/AHS/ASC *Structures, Structural Dynamics and Materials Conference and Exhibit*, AIAA Paper, Atlanta, USA, April, 2000.

DOI: 10.2514/6.2000-1573

[18] Badeau, R., David, B. and Richard, G. L., "Fast Approximated Power Iteration Subspace Tracking", *IEEE Transaction on Signal Processing*, Vol. 53, No, 8, 2005, pp. 2931-2941.

DOI: 10.1109/tsp.2005.850378

[19] Hamada, Y., Ohtani, T., Kida, T. and Nagashio, T., "Synthesis of a linearly interpolated gain scheduling controller for large flexible spacecraft ETS-VIII", *Control Engineering Practice*, Vol. 19, No. 6, 2011, pp. 611-625.

DOI: 10.1016/j.conengprac.2011.02.005

[20] Nagashio, T., Kida, T., Ohtani, T. and Hamada, Y., "Design and Implementation of Robust Symmetric Attitude Controller for ETS-VIII Spacecraft", *Control Engineering Practice*, Vol. 18, No. 12, 2010, pp. 1440-1451.

DOI: 10.1016/j.conengprac.2009.05.003

[21] Tasker, F., Bosse, A. and Fisher, S., "Real-time modal parameter estimation using subspace methods: theory", *Mechanical Systems and Signal Processing*, Vol. 12, No. 6, 1998, pp. 797-808.

DOI: 10.1006/mssp.1998.0161

Appendix A: A data pre-processing way of I-O data for FAPI algorithm

For the establishment of the input vector ξ in FAPI algorithm, there are several methods. Here we introduce a way to construct the vector ξ by the URV matrix decomposition. The detailed procedures of this method are described in reference [21]. Firstly, the Hankel matrix $U(k)$ for input $u(k)$ is written as:

$$U(k) = \begin{bmatrix} u(1) & u(2) & \cdots & u(k) \\ u(2) & u(3) & \cdots & u(k+1) \\ \vdots & \vdots & \ddots & \vdots \\ u(M) & u(M+1) & \cdots & u(k+M-1) \end{bmatrix} \quad (A.1)$$

and the Hankel matrix $Y(k)$ for output $y(k)$ is formulated similarly. The parameter M should be chosen to ensure that the

rank of the Hankel matrix is not less than the system order n. Now, define the Hankel matrices for the next time step $k+1$ as:

$$U(k+1) = \begin{bmatrix} U(k) & u_M(k+1) \end{bmatrix}, Y(k+1) = \begin{bmatrix} Y(k) & y_M(k+1) \end{bmatrix} \qquad (A.2)$$

By the URV matrix decomposition [21], the recursive update for $U(k)$ can be expressed as:

$$(U(k)U^T(k))^{-1} = (U(k-1)U^T(k-1) + u_M(k)u_M^T(k))^{-1}$$
$$= (U(k-1)U^T(k-1))^{-1} - \frac{\gamma(k)u_M^T(k)(U(k-1)U^T(k-1))^{-1}}{1+\alpha(k)} \qquad (A.3)$$

where the parameters $\gamma(k)$ and $\alpha(k)$ are defined as

$$\gamma(k) = [U(k-1)U^T(k-1)]^{-1}u_M(k), \quad \alpha(k) = u_M^T(k)\gamma(k) \qquad (A.4)$$

and

$$U^\perp(k) = I - U^T(k)[U(k)U^T(k)]^{-1}U(k) \qquad (A.5)$$

Then, the following is true:

$$U^T(k)[U(k)U^T(k)]U(k) = I - U^\perp(k)$$
$$= \begin{bmatrix} I-U^\perp(k-1) & 0 \\ 0 & 0 \end{bmatrix} - \begin{bmatrix} U^T(k)\gamma(k)\gamma^T(k)U(k-1)/(1+\alpha(k)) & -U^T(k-1)\gamma(k)/(1+\alpha(k)) \\ \gamma^T(k)U(k-1)/(1+\alpha(k)) & -\alpha(k)/(1+\alpha(k)) \end{bmatrix} \qquad (A.6)$$

leading to:

$$U^\perp(k) = \begin{bmatrix} U^\perp(k-1) & 0 \\ 0 & 0 \end{bmatrix} - \frac{1}{\sqrt{1+\alpha(k)}} \begin{Bmatrix} U^T(k-1)\gamma(k) \\ -1 \end{Bmatrix} \lfloor \gamma^T(k)U(k-1) \quad -1 \rfloor (1/\sqrt{1+\alpha(k)}) \qquad (A.7)$$

where the notation '$\lfloor \ \rfloor$' denotes a double floor. Therefore:

$$Y(k)U^\perp(k) = \begin{bmatrix} Y(k-1) & y_M(k) \end{bmatrix} (\begin{bmatrix} U^\perp(k-1) & 0 \\ 0 & 0 \end{bmatrix}$$
$$- \frac{1}{\sqrt{1+\alpha(k)}} \begin{Bmatrix} U^T(k-1)\gamma(k) \\ -1 \end{Bmatrix} \lfloor \gamma^T(k)U(k-1) \quad -1 \rfloor (1/\sqrt{1+\alpha(k)})) \qquad (A.8)$$
$$= \begin{bmatrix} Y(k-1)U^\perp(k-1) & 0 \end{bmatrix} + \xi(k) \lfloor w^T(k) \quad -1 \rfloor$$

with:

$$z(k) = ([Y(k-1)U^\dagger(k-1)]u_M(k) - y_M(k)) / \sqrt{1+\alpha(k)} \qquad (A.9)$$

$$w^T(k) = \gamma^T(k)U^T(k-1) = u_M^T(k)[U(k-1)U^T(k-1)]^{-1}U^T(k-1) / \sqrt{1+\alpha(k)} \qquad (A.10)$$

and the data updating of $Y(k-1)U^\dagger(k-1)$ and $U(k\text{-}1)U^T(k\text{-}1)$ in equations (A.9) and (A.10) are expressed respectively as:

$$[Y(k)U^\dagger(k)] = [Y(k-1)U^\dagger(k-1)] - z(k)\gamma^T(k) \qquad (A.11)$$

$$[U(k)U^T(k)]^{-1} = [U(k-1)U^T(k-1)]^{-1} - \gamma(k)\gamma^T(k) / \sqrt{1+\alpha(k)} \qquad (A.12)$$

Note that the detailed recursive procedures of $U(k)$ $U^T(k)$ and $Y(k)U^\dagger(k)$ are omitted here; the detailed procedures of this method are described in reference [21]. The vector $z(k)$, which is derived from equation (A.9), is what we need to the FAPI algorithm as the vector $\xi(k)$. When the data vector $\xi(k)$ is obtained, the matrix $\Gamma(k)$ can be derived by the FAPI method in Section 3.

194